Materials and Structures (2022)55:164
https://doi.org/10.1617/s11527-022-02003-w

ORIGINAL ARTICLE

Effect of gamma irradiation on the mechanical properties of carbonation reaction products in mortar

Daria Jóźwiak-Niedźwiedzka · Mariusz Dąbrowski · Kinga Dziedzic · Dariusz Jarząbek · Aneta Antolik · Piotr Denis · Michał A. Glinicki

Received: 17 February 2022 / Accepted: 28 June 2022

Abstract Prediction of carbonation progress in concrete exposed to ionizing radiation is important for the durability assessment of nuclear power plants, eventually needed for operational license extension. The objective of this work is to reveal the influence of gamma irradiation on the carbonation development and resulting microstructural features of cement mortar. The composition of mortar was varied by using mineral additions. Canned specimens at elevated CO_2 concentration environment were exposed to gamma irradiation up to the absorbed dose of 1.6 MGy in the vicinity of spent nuclear fuel rods in pool of research reactor. Micromechanical properties of carbonation reaction products were determined using nanoindentation tests. The carbonation depth was found to increase with increasing absorbed γ dose. The size of calcite crystals was about three times greater in irradiated specimens. Gamma irradiation improved the micromechanical properties of carbonation products. Effects of mineral additives on the characteristics of irradiated mortar are discussed.

Keywords Calcite · Carbonation · Cement mortar · Gamma irradiation · Microstructure · Mineral additions · Nanoindentation

D. Jóźwiak-Niedźwiedzka (✉) · M. Dąbrowski · K. Dziedzic · D. Jarząbek · A. Antolik · P. Denis · M. A. Glinicki
Institute of Fundamental Technological Research Polish Academy of Sciences, Pawińskiego 5b, 02-106 Warsaw, Poland
e-mail: djozwiak@ippt.pan.pl

M. Dąbrowski
e-mail: mdabrow@ippt.pan.pl

K. Dziedzic
e-mail: kdzie@ippt.pan.pl

D. Jarząbek
e-mail: djarz@ippt.pan.pl

A. Antolik
e-mail: aantolik@ippt.pan.pl

P. Denis
e-mail: pdenis@ippt.pan.pl

M. A. Glinicki
e-mail: mglinic@ippt.pan.pl

Published online: 12 July 2022

1 Introduction

The significance of concrete carbonation phenomenon for the durability of concrete structures at nuclear power plants is recognized in design and maintenance guidelines [1, 2]. Electricity providers perform required structural condition monitoring by sampling at most exposed locations to predict the progress of carbonation in concrete. For a typical concrete mix in nuclear power plants (NPP) in Japan, the prediction of carbonation depth is feasible using the AIJ formula [3]. The progress of carbonation is influenced both by the concrete mix design and the environmental exposure conditions, including CO_2 concentration in

the air and the moisture state of concrete. It is commonly assumed that for 40–50% RH, the carbonation rate is medium, for 60–70% RH, carbonation rate is high [2, 4, 5]. The role of increased temperature in accelerated carbonation tests of concrete of "typical" composition for NPP structures was studied by Mitsugi et al. [3]. It was found that the environmental parameters (temperature, relative humidity) were different for carbonation progress and for steel rebar corrosion progress. It is due to the fact that the humidity environments where carbonation progresses and the temperature environments where rebar corrosion progresses do not correspond with each other, rebars are typically unlikely to corrode even if carbonation has reached the rebars, provided they are not subjected to extreme wet-dry cycles. Another specific environmental condition potentially causing a degradation of concrete in NPP structures is ionizing radiation and therefore it should be included in the carbonation studies. However, the evaluation of such concrete property changes is challenging [6] because of the limited number and size of specimens in accelerated irradiation experiments.

According to previous accelerated irradiation experiments, summarized by Field et al. [7], concrete properties were found to deteriorate under neutron and gamma irradiation. The irradiation induced strength reduction was clearly evident beyond the gamma dose threshold of 2.0×10^{10} rad (2.0×10^{8} Gy) which has been suggested by Kontani et al. [8], however an increased temperature and other test conditions are considered as important influencing factors, too. A review of test conditions for accelerated studies of gamma irradiation are summarized in [9]. For lower gamma doses up to 40 kGy a reduction of capillary porosity and pore size refinement in hardening cement mortar was found. Gamma irradiation of hardening cement mortar, starting before initial setting time, resulted in an increase of the flexural and compressive strength by 71 or 102%, respectively. Also an increased presence of portlandite was found. Mechanical properties of calcium silicate hydrates were examined with nanoindentation after gamma-adsorbed doses up to 0.784 MGy, and neither elastic modulus nor stress relaxation tests showed any apparent trend with irradiation dose [10]. Reches [11] concluded that gamma radiation does not have a significant effect on the compressive or flexural strength and on the modulus of elasticity of cement-based composites. Hilloulin et al. [12] revealed that Young's modulus of irradiated (up to 0.257 MGy) specimens did not significantly differ from the one of control specimens. Soo and Milian [13] analyzed the influence of the dose rate on the compressive strength of Portland cement based materials at 10 °C, revealing that the strength of the irradiated materials exposed to rather low dose rate 31 Gy/h failed rapidly once the total dose exceeded about 0.1 MGy. But when exposing the same materials to higher dose rate 380 kGy/h led to an increase in mechanical strength [14].

There are only few data on the influence of low-dose gamma irradiation on the rate of carbonation of cement-based materials, [15–18]. Vodák et al. [15] applied the maximal gamma dose 1 MGy on hardened cement paste (w/c = 0.4) and revealed that radiation at least accelerated carbonation and besides natural carbonation there was also independent carbonation caused by γ-irradiation. They showed a decrease of the average pore diameter due radiation-induced carbonation and they assumed that the natural carbonation acted in the surface layer, while the carbonation due to irradiation took part within the entire material. Barnes et al. [16] also studied γ-irradiation effects on hardened cement paste and revealed that an integral dose of 10^{7} Gy during a period of approximately 6 months was found to increase carbonation for the irradiated specimens. They analyzed cementitious paste (w/c ratio 0.30 and 0.45) which was exposed to gamma dose of 10^{7} Gy during a half a year. They confirmed that the depth of carbonation significantly increased for irradiated specimens compared to non-irradiated specimens. The enhanced carbonation was associated with the dehydration due to radiolysis of pore water in the paste, [16]. Bykov et al. [17] observed the effect of gamma-ray irradiation on the occurrence of cement paste carbonation. Increasing the radiation dose up to 3.2 MGy lead to an increase in the concentration of calcium carbonate in Portland cement specimens. The phase content of $CaCO_3$ (orthorhombic and rombohedra) in cement from Rietveld calculation increased about 65%, [17]. Vodák et al. [15] showed that the proportion of calcite to portlandite increased due to gamma irradiation. Maruyama et al. [18] revealed that calcite was mainly formed in the specimens exposed to the room atmosphere without irradiation, while vaterite and aragonite were found in the irradiated specimens. They concluded that the calcite is formed by the

transformation of metastable vaterite because the specimen that dried quicker is thought to exhibit more vaterite. During their irradiation process, specimen temperature was increased as a result of gamma-ray heating (more than 5 °C) and, consequently, the specimen was dried.

Due to the need to shorten the test duration, accelerated carbonation tests are used, where the CO_2 concentration and thus the carbonation rate are much higher than under atmospheric conditions, [19]. The carbonation ingress rate under higher CO_2 concentrations than the atmospheric level has been reported to deviate from the rate implied by uniform Fickian diffusion, [19]. Finding the correlation between the natural and accelerated carbonation effects of cement-based materials is still the subject of many studies [20–22]. Previously, the diffusion rate of CO_2 was assumed to be constant, but more specific assumptions were made in the new models described in [19, 22–24]. Many factors are taken into account, including the degree of hydration, porosity, CO_2 concentration, relative humidity, amounts and types of microscopic phases or microstructural features which determine the rate of CO_2 diffusion. However, so far none of the models has considered the influence of gamma irradiation on the carbonation process of cement-based materials, but it could be estimated on the basis of microstructure analysis—crystal size and micromechanical properties of $CaCO_3$.

Effects of long term gamma irradiation on in-service concrete structures used for nuclear waste storage were reported by Potts et al. [25]. In contrast to accelerated irradiation studies, the exposure to 35.8 MGy did not result in a reduction of compressive strength. Phenolphthalein indicator tests revealed quite a small degree of carbonation of in-service specimens, that was explained by a very limited amount of air surrounding them during a long-term storage inside the waste facility.

Previous studies indicated that substantial damage to concrete would only occur for gamma doses of the order of 10^8 Gy, [8, 13, 26]. However, there has been little attempt to determine the influence of lower dose of gamma irradiation influences on concrete microstructure and properties [12, 27] or whether it is an important factor in concrete degradation. The aim of the investigation is to reveal the influence of low-dose gamma irradiation on the mechanical properties carbonation reaction products in mortar. The range of tested materials include Portland cement mortar modified with mineral additives. Companion tests were conducted at the elevated temperature to gain insight into comparative effects on carbonation process and microstructural features of mortar.

2 Materials and test conditions

In all mortar mixes as a fine aggregate, standard natural siliceous sand according to PN-EN 196-1 [28] (specific gravity equal to 2.65 g/cm^3 and maximum grain size of 2 mm) and tap water were used. The differentiation of carbonation depending on the variability of the chemical composition was taken into account, therefore the tested materials include Portland cement mortar modified with mineral additives, such as fly ash or limestone powder. Portland cement CEM I 52.5 R (PN-EN 197-1 [29]), siliceous fly ash class A (PN-EN 450-1 [30]) and limestone powder (PN-EN 197-1 [29]) were used. Their chemical composition and physical properties are given in Table 1. The 20% or 40% of cement volume was replaced by fly ash or limestone powder. Specimens were marked R0—reference, R20V, R40V with fly ash and R20LL, R40LL with limestone powder. The constant water/binder ratio equal to 0.6 was maintained. The specimens were made with a high water-cement ratio in order to distinguish the effect of radiation from the maturation of the mortars. Three prisms (40 × 40 × 160 mm) for each composition were cast. Also cylinders with diameter of 100 mm and height of 150 mm were cast for additional carbonation test. All specimens were cured in water at the temperature of 20 ± 1 °C for 28 days before testing. A large single crystal of calcite with the size of few centimeters was used as a reference material for micromechanical studies. The crystal was locally collected in Poland.

In order to determine the influence of gamma irradiation on the mortar carbonation, two types of testing conditions were adopted: (1) specimens stored in sealed containers in a pool with spent fuel in working research reactor (named-irradiated), and (2) specimens of the same composition, also stored in sealed containers but in a laboratory tub (named non-irradiated). The test conditions were designed to obtain differentiation not only due to the composition of the mortars but also the initiated carbonation

Table 1 Chemical composition (XRF, chemical methods) and physical properties of cement, fly ash and limestone powder

Constituent	CEM I 52.5R	Fly ash	Limestone powder
SiO_2, %	20.10	52.00	6.26
CaO, %	63.70	1.10	48.39
Al_2O_3, %	4.70	30.10	2.06
Fe_2O_3, %	2.80	6.69	1.58
MgO, %	1.30	2.72	1.58
SO_3, %	2.70	0.33	0.26
K_2O, %	0.80	3.16	0.29
Na_2O, %	0.10	1.47	0.10
Cl^-, %	0.05	0.01	0.01
Loss of ignition, %	3.30	2.37	39.11
Blaine specific surface, cm^2/g	4500	2250	8000
Density, g/cm^3	3.10	2.16	2.62
Activity index, %	–	K_{28} 80.3	–
		K_{90} 97.0	

process. From literature [16] it is known that in sealed specimens (w/c ratio of 0.45) that were not subjected to either free atmospheric conditions or irradiation, no carbonation was detected. Therefore, the tested mortar specimens were placed in tight containers filled with 1% CO_2 and constant RH = 50% ± 10%. The gas was already in the cans, without any additional flow. A superabsorbent polymer was used to ensure constant humidity.

Spent fuel rods which are stored in a dedicated pool next to the research reactor were used as the source of gamma irradiation. A high flux Polish research reactor, which is a water and beryllium moderated reactor of a pool type with graphite reflector and pressurised channels containing concentric six-tube assemblies of fuel elements was used, [31]. Nominal power is 30 MW (thermal), thermal neutron flux is $3{\cdot}10^{14}$ n/s cm^2 and fast neutron flux $1{\cdot}10^{14}$ n/s cm^2.

Each of the sealed protective containers containing mortar prism was placed in a sterilization container which in turn was placed in a spent fuel pool, as close as possible to the spent fuel elements. Temperature markers were individually attached to the backsheet of the containers. A thermoluminescent dosimeters (TLD meters) MCP-N were mounted on the top and bottom surfaces of the protective sealed containers. The analysis of the results were performed using the UHTR method (the ultra-high temperature ratio) [32]. The determined amount of the dose absorbed in water is the average value of the readings of two dose meters attached to the walls of protective containers. The maximum dose absorbed in water was estimated to be 1.6 MGy.

The preliminary tests showed that the temperature of the water in the pool was around 40 °C, so such temperature was assumed in the laboratory tub (non-irradiated specimens). During the experiment the RH and temperature values were recorded using the iButtons, which were placed next to mortar prisms in the sealed containers in a laboratory tub. The summary of the thermal and humidity conditions measured during the tests is presented in Table 2.

Additionally, a series of specimens were left in free atmospheric conditions at temperature 20 ± 2 °C and RH = 50% ± 10% (named-laboratory conditions), during the same period as stored in a spent fuel pool.

3 Test methods

3.1 The carbonation depth

The carbonation depth was determined on the freshly broken surface of the mortar prisms. Specimens were tested at the same time after being in the spent fuel pool for 10 months. The depth of carbonation was determined with phenolphthalein (Fig. 1) and estimated on the photographs, with an accuracy of 0.01 mm (Fig. 1a and b). For the further analysis the mean value of 20 measurements from each fracture

Table 2 The summary of the thermal and humidity conditions in sealed containers and in the laboratory

Specimen	Temperature °C	Relative humidity %	Initial CO_2 concentration %
Gamma irradiated	40 ± 3.0	N/A	1 ± 0.2
Non-irradiated	40 ± 0.6	59 ± 4.5	1 ± 0.2
Laboratory conditions	23 ± 1.0	43 ± 5.0	0.04

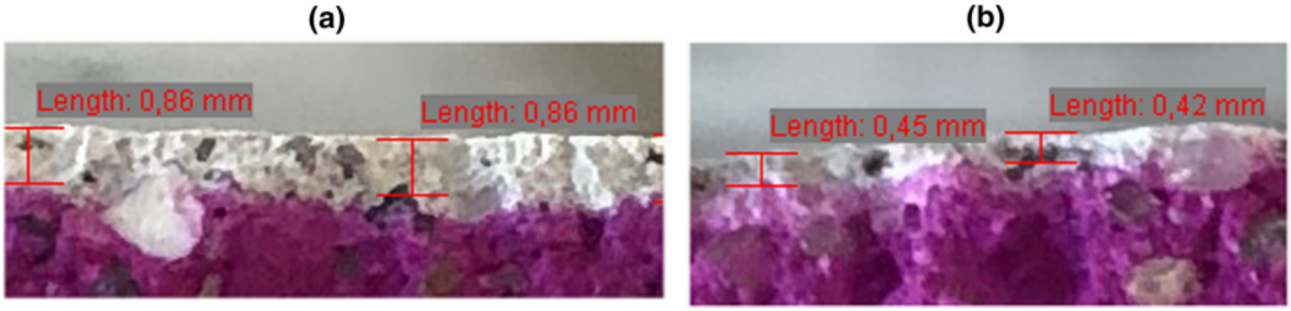

Fig. 1 The carbonation depth determined with phenolphthalein on freshly split surface: **a** reference mortar R0 after gamma irradiation (spent fuel pool), **b** reference mortar R0 without gamma irradiation (non-irradiated, from the chamber)

surface was used. In parallel, the carbonation depth was determined on specimens in CSM climatic chamber at constant concentration of CO_2 (1%) at 22 °C and 60% relative humidity. The depth of carbonation was examined on the freshly split surface (cylinder, height 150 mm and diameter 100 mm) with phenolphthalein solution after 0 and 28 days of CO_2 exposure according to PN-EN 13295 [33]. The carbonation depth was determined also after 55 and 316 days of CO_2 exposure which corresponded to the beginning and end of storing specimens in the pool with spent fuel.

3.2 X-ray diffraction analysis

The outer layer, up to a depth of approx. 3 mm, was taken from mortar specimens for analysis of the mineral composition using X-ray diffraction method (XRD). They were powdered and sieved through a 0.045 mm sieve. The Bruker D8 DISCOVER diffractometer was used with a voltage of 40 kV and 40 mA lamp current. Copper lamp was used as an X-ray source. The diffraction patterns were collected over a 2θ range from 5° to 70° with a 1°/min step by flat plane geometry. The Diffrac.Eva V5.2 software was used to evaluate the XRD patterns and to determine the crystallite phases. Reference specimens R0 and with 40% of limestone powder R40LL or fly ash R40V, irradiated and non-irradiated were investigated.

3.3 Microstructure analysis

Evaluation of the microstructure was performed using a combination of scanning electron microscopy (SEM) in the back scattered electrons (BSE), the secondary electrons (SE) modes and Energy Dispersive X-ray analysis (EDX) on irradiated specimens (stored in a pool with spent fuel) and non-irradiated specimens (stored under the same conditions, without radiation).

The effect of gamma irradiation (SEM as well as nanoindentation) was tested on specimens irradiated to the highest dose of about 1.6 MGy.The analysis was carried out on specimens without and with additions used as 40% of cement replacement. Specimens for SE mode were pieces of mortar broken off from an adjacent location with a fresh fracture surface including an outer surface of the specimen. The specimens for the BSE mode were obtained by slicing mortar specimens with a slow speed diamond saw. The specimens 50 × 30 × 15 mm were dried at 50 °C for 3 days, vacuum-impregnated with a low-viscosity epoxy, lapped and polished using a special procedure for SEM specimens. Each specimen was prepared in such a way that the polished face which was to be examined was a cut surface from the edge of the bar.

The specimens were coated with carbon and a strip of conductive tape has been attached to each specimen. Each of the specimen was thoroughly examined using JEOL JSM-6380 LA SEM–EDX using an acceleration voltage of 15 kV.

3.4 Mechanical properties of calcite

The mechanical properties of calcite were measured using nanoindentation method. Calcite crystals located in the outer layer of the specimens, from 0 to approx. 5 ÷ 6 μm, were subjected to the nanoindentation test. Before each indent, a SEM–EDS analysis was performed to verify the calcite composition. Nanohardness tests were conducted by an in-situ Alemnis indentation tester equipped with diamond Berkovich tip placed inside the Zeiss Crossbeam 350 chamber. The maximum force was 30 mN. The load control was applied. The speed of both loading and unloading was equal to 1 mN/s. After reaching the maximum force, the indenter was held for 10 s. In order to determine the exact values of hardness and Young's modulus from the indentation curves Olivier-Pharr [34] method was used. The results are the average of at least 10 measurements for each mortar.

3.5 Mechanical properties of mortar

Mechanical tests were conducted on mortar beams 40 × 40 × 160 mm. The dynamic modulus of elasticity (E_{dyn}) and flexural strength (f_t) were determined on three bar specimens, while the compressive strength (f_c) was tested on four halves of the bars. Tests were carried out for each of the three types of specimens storage (pool, similar to the pool but without radiation and laboratory conditions). E_{dyn} was determined using GrindoSonic apparatus, which gives the frequency of a vibration created by slight shock on the specimen and the elastic modulus was calculated from this frequency with the Spinner and Teft [35] model. Three point bending test was used to determine the flexural strength. The external load P was applied in the mid-span of the specimen through a loading machine, having a load capacity of 50 kN. Tests were performed by controlling the displacement of the loading cell, whose stroke moved at a velocity of 50 N/s. Compressive load was applied by using a 2000 kN capacity universal testing machine at the loading rate of 500 N/s. Flexural and compressive strength was determined according to PN-EN 196-1 [28].

4 Test results

4.1 Carbonation depth

Changes in the carbonation depth in the mortar under the influence of gamma radiation are shown in Fig. 2. The results concerning mortars stored under reference conditions (non-irradiated) and in laboratory conditions are also presented. It was found that gamma irradiation increased the carbonation depth (Fig. 1) in all the mortar specimens. In the reference mortar the increase of carbonation depth due to the γ irradiation was 125%. In irradiated specimens containing 40% of mineral additions, slightly greater increase of carbonation depth was determined in specimens containing limestone powder (41%) compared to fly ash (31%), but in both cases a linear shift in the carbonation depth in the mortars subjected to radiation is visible.

Figure 2 shows the results of the carbonation depth of mortars tested in three different conditions: after gamma irradiation (irradiated, spent fuel pool), without gamma irradiation (non-irradiated, from the chamber), without gamma irradiation (non-irradiated, from the laboratory conditions). Figure 3 shows the results of a standard carbonation test performed on a mortar.

As it was expected, the influence of mineral admixtures on carbonation depth is visible. As in the standard tests, Fig. 3, there is a correlation between the replacement of a part of the cement by limestone powder or fly ash. The higher content of cement replacement, the higher the carbonation depth. Above correlation is more evident in specimens tested under laboratory conditions (Fig. 2). This is probably due to the conditions of testing the specimens, in the pool and under the same conditions without gamma irradiation, where the specimens were closed in airtight containers. So the available CO_2 was consumed after some time. However, the influence of both the additive content and the gamma radiation is visible.

A standard carbonation test procedure was also performed to verify the effect of the mineral additives. As expected [36, 37] the depth of carbonation increased with time and increased with increasing the cement replacement, 20 and 40% by limestone

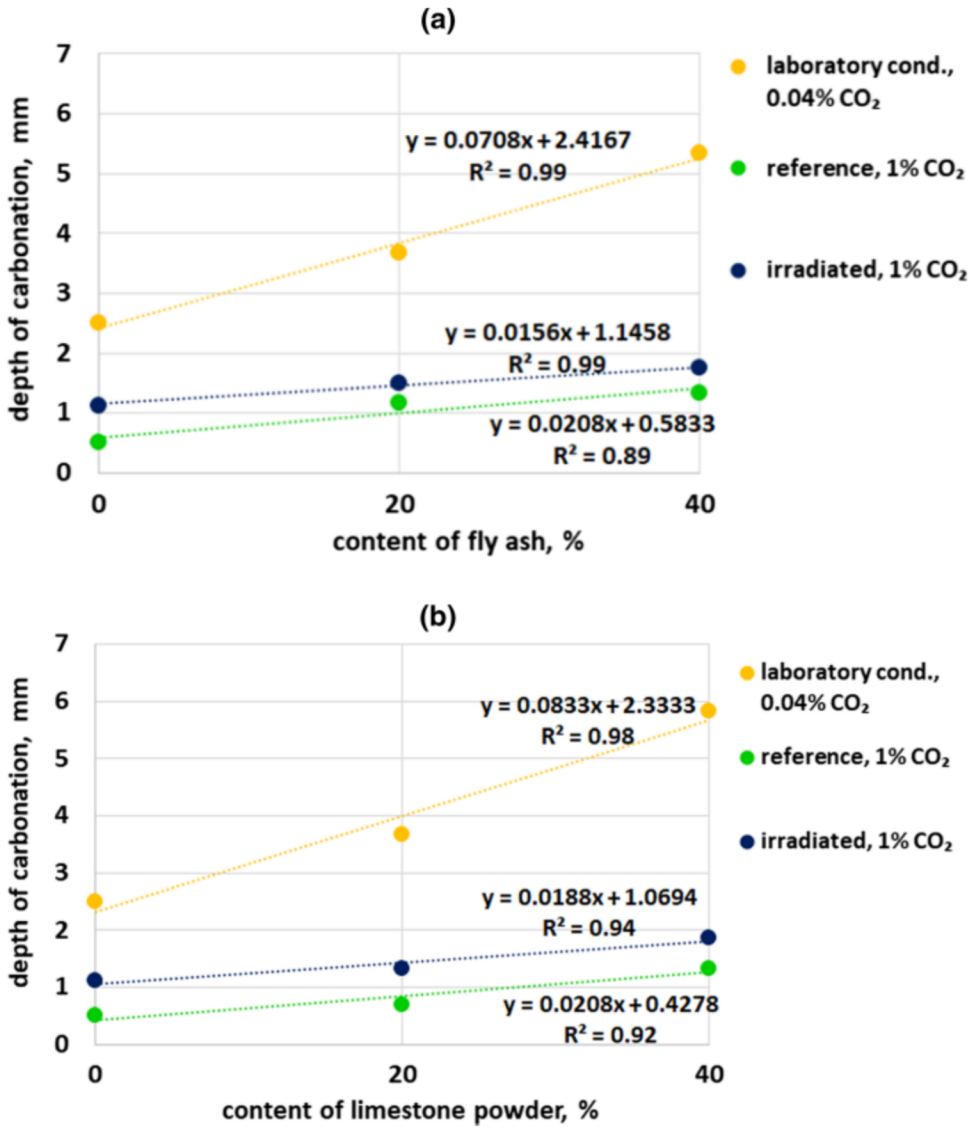

Fig. 2 Influence of replacing cement with mineral additive and CO_2 exposure conditions on the carbonation depth in mortar: **a** fly ash, **b** limestone powder

powder or fly ash, Fig. 3. When replacing 20% of cement, the difference in carbonation depth between limestone powder and fly ash is not significant, 18 and 15 mm respectively, but when using 40%, a considerable increase in carbonation is seen for limestone powder, 50 mm compared to 30 mm in mortar with 40% of fly ash.

4.2 Microstructural observations

The results of microscopic observations performed on mortar specimens exposed and non-exposed to γ-irradiation are presented in Figs. 4, 5, 6. The major gamma irradiation induced changes were visible in an external layer of the specimens, up to 1 mm from the edge of specimens subjected to irradiation. Clear differences in the size of calcite crystals are visible, Fig. 4. Calcite crystals formed on the surface of specimens subjected to gamma irradiation are approx. 15 μm dimension while in non-irradiated specimens about 5 μm. It can also be seen that the calcite crystals formed on the non-irradiated specimens are of similar size and shape, like elongated columnar, while on the irradiated specimens have non regular shapes, like mosaic, which may indicate the higher crystal growth rate, [38]. A uniform compact layer of calcite in all specimens containing mineral additives under gamma radiation was found (Fig. 5b), while in non-irradiated

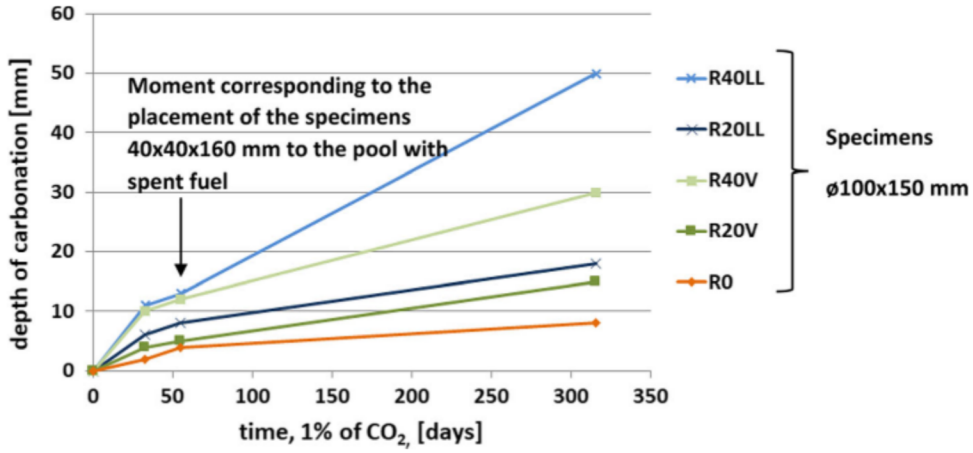

Fig. 3 Depth of carbonation vs time, standard test [33]

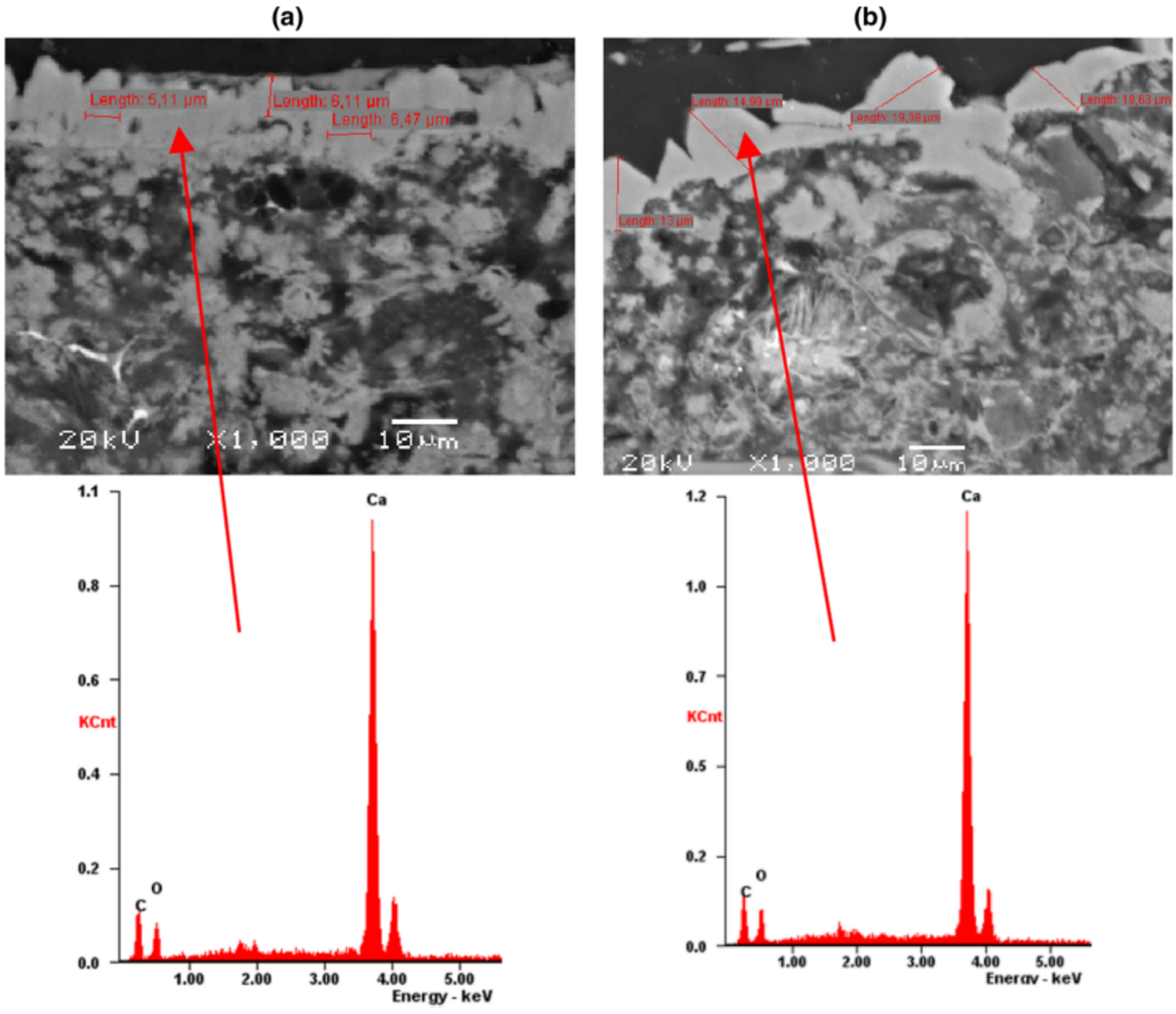

Fig. 4 SEM-BSE images of polished specimens without any addition, outer surface of the specimen, EDS analysis showing $CaCO_3$: **a** without irradiation, **b** after gamma irradiation

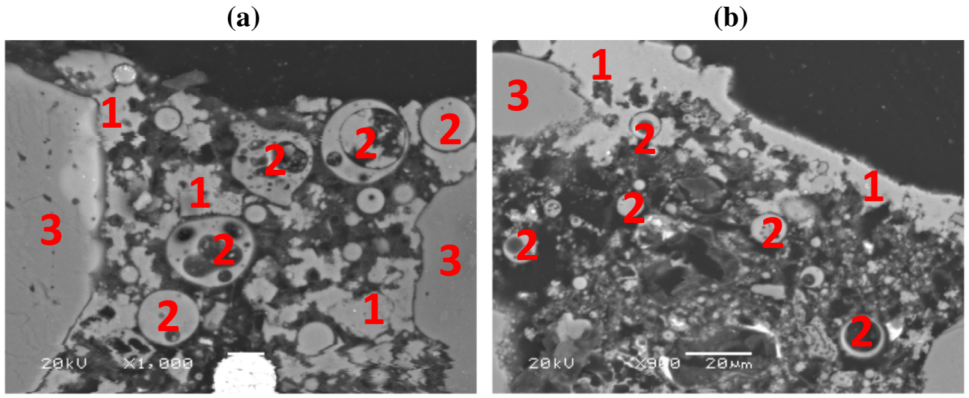

Fig. 5 SEM-BSE images of polished specimens with 40% of fly ash, outer surface of the specimen: **a** without irradiation, **b** after gamma irradiation; 1-calcite, 2-fly ash, 3-sand grain

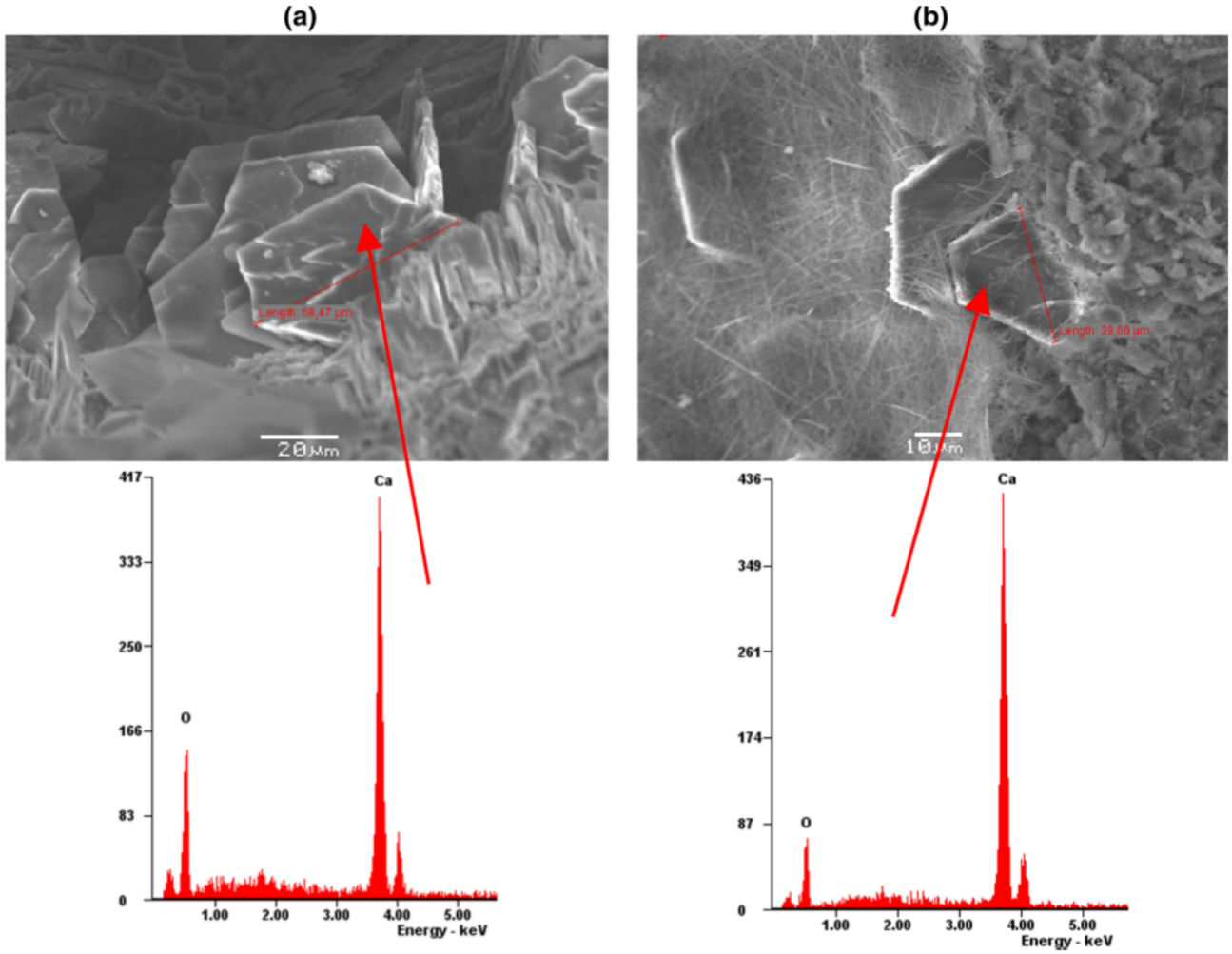

Fig. 6 SEM-SE (secondary electrons) images of specimens with 40% of fly ash with EDS analysis showing portlandite plates, about 500 µm form the surface of the specimen: **a** after gamma irradiation, **b** without irradiation

specimens only a local carbonation was noticed (Fig. 5a). Examination of SEM-SE images revealed larger portlandite plates in specimens under gamma irradiation. Average dimension of single crystal was about 60 μm for irradiated and about 30 μm for non-irradiated specimens, Fig. 6. Also C–S–H was characterized by more needle structure (Fig. 6b) in non-irradiated specimens, regardless of their composition.

Also in the irradiated specimens stored in the spent fuel pool, depending on the depth from the surface, differences in the microstructure in terms of porosity, cement grains and the presence of microcracks and monosulfate are visible. The area of increased porosity in the surface zone at a depth of max. 1 mm is clearly visible. These are not characteristic air pores, rather it looks like empty spaces with irregular shapes.

Figure 7 shows diffraction patterns of analysed reference mortar specimens non-irradiated and after exposure to γ-radiation with dose in the range up to 2 MGy. The stronger diffraction peaks of calcite (3.03 Å) and portlandite (4.9 Å) are shown. Although, the mineral composition obtained using the X-ray diffraction analysis of the irradiated and the control specimens was similar, the effect of irradiation on carbonation was noticeable. After the γ-irradiation an increase in the concentration of calcium carbonate was found which is equated with larger carbonation. In addition, after gamma irradiation the lower the concentration of the portlandite phase was present which is consistent with the results of the increase of calcite. Within the analysis the strongest diffraction peaks of calcite, the increase of calcite intensity was found in the irradiated mortars, about 80%, 90% and 60% for R0, R40LL and R40V, respectively. At the same time, the reduction of the portlandite intensity amounted to about 50, 70 and 30%, respectively. No other carbonation products like aragonite or vaterite were found.

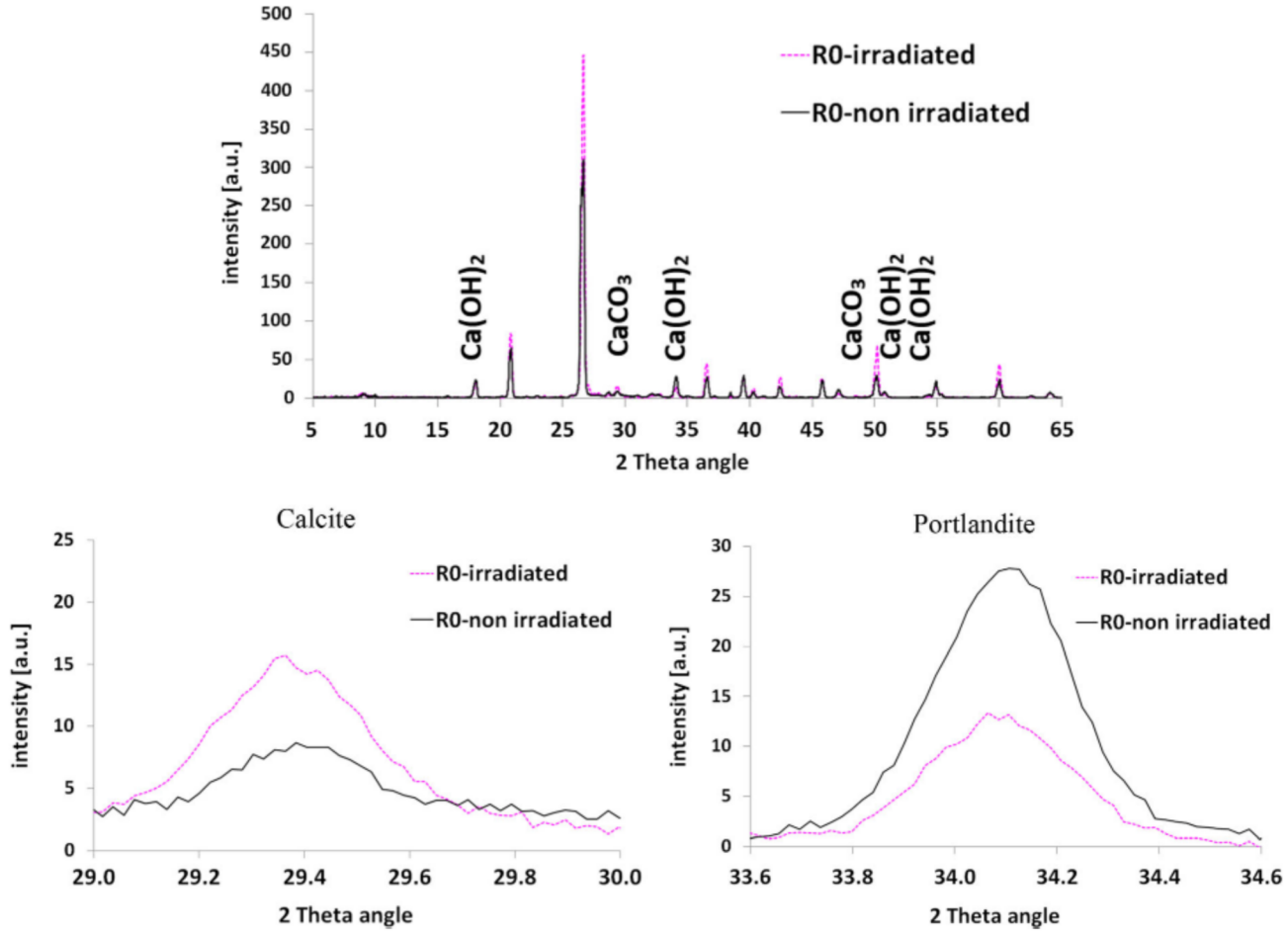

Fig. 7 XRD patterns of Portland cement mortars R0 after irradiation and non-irradiated

Table 3 The nanoindentation test results in calcite at constant force of 30 mN

Specimen	Displacement		Nanohardness		Young's modulus	
	[nm]		[GPa]		[GPa]	
	Non-irradiated	Irradiated	Non-irradiated	Irradiated	Non-irradiated	Irradiated
Reference (no additions) R0	730	352	3 ± 0.5	24 ± 3	58 ± 4	90 ± 5
40% of fly ash R40V	1295	382	2 ± 0.5	12 ± 0.5	45 ± 4	51 ± 6
40% of limestone powder R40LL	865	N/A	2 ± 0.4	N/A	39 ± 5	N/A
Calcite-mineral	745	–	2 ± 0.05	–	60 ± 1	–

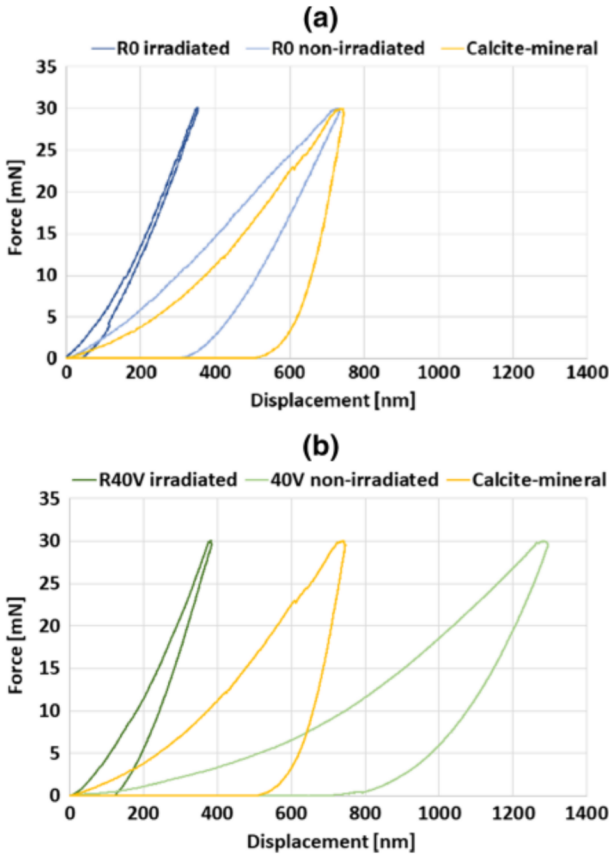

Fig. 8 Nanoindentation load–displacement relationship for calcite in mortar subjected to irradiation and without irradiation and calcite-mineral without irradiation: **a** reference mortar and **b** mortar with 40% of fly ash

4.3 Micromechanical properties of calcite formed in mortar

In Table 3 the summary of the nanoindentation results in calcite is shown. The differences in the shape of load–displacement curves for gamma irradiated and non-irradiated are illustrated in Fig. 8 Reference curves obtained for pristine calcite mineral are also presented. Unfortunately, the surface of the irradiated specimen R40LL was damaged and it was not possible to carry out the nanoindentation test.

A significant influence of γ irradiation on calcite nanohardness is found. With the application of the same force 30mN the displacement of the indenter in the specimens subjected to gamma irradiation was much smaller than in the specimens without irradiation, Fig. 8a and b, which proves their higher values of nanohardness. The maximum indenter displacement for the calcite in the reference mortar R0 without irradiation and for the calcite-reference mineral were quite the same size, 730 nm and 745 nm respectively. For the calcite in mortar with 40% of fly ash, the nanohardness after irradiation was six times higher than without irradiation, 12 ± 0.5 and 2 ± 0.5 GPa, respectively. As the hardness of calcite increased after irradiation, the Young's modulus also increased by more than 50% for mortar without additions and about 13% for the mortar containing 40% of fly ash. The elastic properties of the non-irradiated calcite-mineral were quite similar as for the calcite in the non-irradiated reference mortar R0, with the range from 58 to 60 GPa. Despite large differences in the values of displacement in non-irradiated specimens from 1275 to 730 nm, all the irradiated specimens showed similar values of max. displacement, about 350–380 nm.

4.4 Mechanical properties of mortar

The results of compressive and flexural strength as well as dynamic modulus of elasticity of tested mortars are shown in Table 4. The irradiated specimens showed slightly lower values of f_t, f_c and E_{dyn} compared to not irradiated specimens, stored in similar

Table 4 Results of the compressive and flexural strength and modulus of elasticity of mortar

			R0	R20LL	R40LL	R20V	R40V
Gamma irradiated	f_c	MPa	54.2 ± 1.4	42.9 ± 2.2	28.8 ± 2.7	47.5 ± 2.1	29.0 ± 2.7
	f_t	MPa	7.9 ± 0.1	7.0 ± 0.2	5.6 ± 0.2	7.9 ± 0.4	6.4 ± 0.3
	E_{dyn}	GPa	24.0 ± 0.5	22.2 ± 0.2	18.9 ± 1.0	22.1 ± 0.1	18.8 ± 0.2
Non-irradiated	f_c	MPa	54.3 ± 2.5	46.0 ± 2.6	30.2 ± 2.0	48.5 ± 2.6	32.3 ± 4.6
	f_t	MPa	8.2 ± 0.3	7.3 ± 0.1	5.7 ± 0.5	8.4 ± 0.1	6.7 ± 0.2
	E_{dyn}	GPa	24.2 ± 0.1	23.1 ± 0.3	19.8 ± 0.3	22.2 ± 0.3	19.5 ± 0.9
Laboratory conditions	f_c	MPa	60.4 ± 2.7	51.3 ± 4.6	34.9 ± 3.1	55.4 ± 1.6	47.6 ± 4.2
	f_t	MPa	8.5 ± 0.2	8.4 ± 0.2	7.0 ± 0.4	8.9 ± 0.3	7.9 ± 0.4
	E_{dyn}	GPa	25.6 ± 0.5	23.4 ± 0.4	19 ± 0.2	23.3 ± 0.6	20.8 ± 1.7

conditions. In the current research (max. 1.6 MGy) and in the studies known from the literature [8, 12, 38, 39], the values of the standard deviation were so large that confirming a linear relationship between gamma dose and compressive/flexural strength is not precise. However the general trend that gamma irradiation reduces the mechanical properties of mortars is noticeable. The irradiation induced reduction of the compressive strength was with the range from 0.1 to 3.1 MPa, the flexural strength from 0.1 to 0.5 MPa and modulus of elasticity from 0.1 to 0.9 GPa. Due to gamma irradiation the largest differences in compressive strength occurred in specimens containing 40% of fly ash, a decrease by 10.3%. The highest reduction in flexural strength was observed in specimens containing 20% fly ash, a decrease about 6% and the largest decrease in the value of the modulus of elasticity was visible in the specimens with 40% of limestone powder, about 5%.

Regardless of the method of storing the specimens, the effect of replacing a part of the cement with 20 or 40% limestone powder or fly ash is clearly visible. With an increase in the content of the additive, the mechanical properties decrease, except when 40% of limestone powder is used. Of all the mortars, those matured in laboratory conditions were characterized by the highest values of mechanical properties.

5 Analysis and discussion

In the conducted research was found that γ-irradiation increased the depth of carbonation. A linear relationship between the depth of carbonation and gamma irradiation was determined, Fig. 9. With the increase of the absorbed gamma dose, the depth of carbonation increased. The above results are in line with the research of Vodák et al. [15] and Bar-Nes et al. [16], however they analysed the Portland cement paste with much lower w/c ratio. In the presented research on the influence of gamma irradiation on the carbonation depth, there is a difference between the specimens containing mineral additives and the reference specimens, Fig. 9, which is due to the reduced content of portlandite and the faster progress of the carbonation process. In the reference mortar the increase of carbonation depth due to the γ irradiation was more than twice, whereas in mortars with 40% of mineral additions was about one third. However, the general trend is maintained, with increasing gamma irradiation dose the depth of carbonation increases.

In the current research the test conditions designed in such a way that the temperature was very close in irradiated and non-irradiated specimens to distinguish the effects of gamma irradiation. It is presumed that for this reason the presence of vaterite was not found in the analysed specimens as it was shown in research by Maruyama et al. [18]. This finding is in line with the observations of Goni et al. [41]. They revealed that during the natural carbonation process of cement-based materials, three varieties of crystalline $CaCO_3$ (calcite, vaterite and aragonite) are produced, but calcite is the main polymorph produced by accelerated carbonation.

All the microstructural observations show the intensification of the carbonation process under the influence of gamma radiation, which confirms the results on the depth of carbonation, Fig. 9. The above

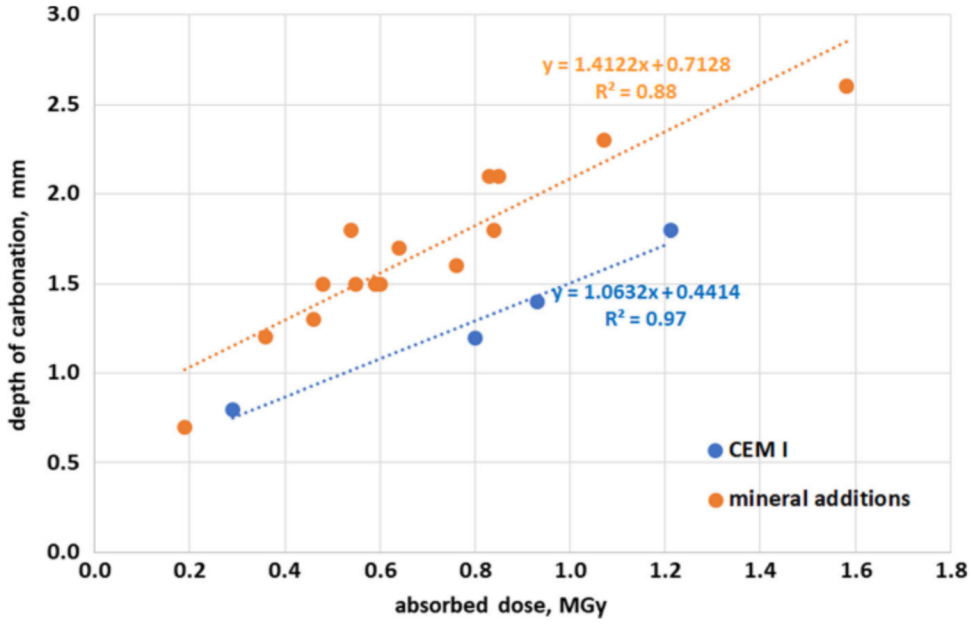

Fig. 9 Influence of gamma dose on the depth of carbonation in mortar with and without mineral additions

statement was confirmed in the literature by Dąbrowski et al. [42]. They demonstrated qualitative effects of gamma early-irradiation in cement matrix in the surface layer up to the depth of 2 mm in concrete by a visible higher degree of cement reaction with no unhydrated cement grains as well as more abundant portlandite crystals. However, Bykov et al. [17] did not find any significant morphological changes in cement paste specimens irradiated up to 3.3 MGy. As well as Maruyama et al. [18] when comparing the FE-SEM images. They did not find any differences between the images of irradiated and reference specimens, but they analysed the broken surface of the specimens where micro-area analysis is not recommended. In the current research an analysis of the polished surface was also performed using SEM in backscattered mode (BSE), Figs. 4 and 5. Also in the presented research the temperature value was the same for the irradiated and non-irradiated specimens (Table 2) and allowed to distinguish the effects of gamma irradiation. The effect of a low dose (up to 56 kGy) of gamma irradiation in the outer layer of the concrete was also observed by Dąbrowski et al. [42]. They found the effects of early γ-irradiation on microstructural features of cement matrix in the subsurface layer up to the depth of 2 mm. Khmurovska et al. [43] revealed that gamma irradiation (up to 15 MGy) lead to the increase in porosity in cement mortar due to the pore structure rearrangement and microcrack occurrence. However, Vodak et al. [40] found that porosity of concrete was decreased under the influence of gamma radiation.

The results on the gamma irradiation effect on the micromechanical properties of calcite are consistent with already presented microstructural features (Figs. 4 and 5) and also with previous research on cement paste and mortar, [12, 15]. Gamma irradiation caused an eightfold increase in calcite nanohardness in the reference specimen and sixfold increase in calcite nanohardness in the specimen containing 40% of fly ash. It was associated with an increase in Young's modulus, by 55% in mortar without additives and by 13% in mortar with 40% fly ash. The obtained nanohardness value for mortar without mineral additions after gamma irradiation was 24 ± 3 GPa which is much higher that the hardness of calcium silicate (C_3S, C_2S) and calcium aluminoferrite (C_4AF) which are similar (between 8 and 9.5 GPa) and even higher that the hardness of C_3A (10.8 GPa), [44]. The gamma dose of 2 MGy was too low to exhibit any influence on calcite embrittlement, although a similar phenomenon is known in metals where radiation leads to the displacements of atoms from their equilibrium lattice sites, causing lattice defects, which are responsible for an increase of hardness but also embrittlement, [45]. Hilloulin et al. [12] revealed that γ-irradiated mortar specimens exhibited greater hardness than references. Vodak et al. [15] showed that the hardness of cement

paste increased with dose of irradiation. However, in the above tests of paste and mortar, due to the large heterogeneity of the material a probable-error-bars was up to 50%. Hughes and Trtik [46] using a by depth-sensing nanoindentation to estimate the micro-mechanical properties of cement paste concluded that the large standard deviation for individual categories of phases and mixtures of phases within the cement paste was the reason that only the most basic conclusion could be reached. In the current research the large-enough calcite phase could be well detected in mortar and the nanoindentation test was performed only in calcite crystals. That ensures proper certainty regarding the micromechanical representation of tested mineral phase. No published data is available for comparison of micromechanical properties of calcite formed under the influence of gamma irradiation. Pignatelli et al. [47] revealed the influence of Ar^{+} ion irradiation on the density reduction of calcite, contrary to the density increase of quartz. These differences were found correlated with the type of bonds in these minerals (predominantly ionic or covalent) and the rigidity of the mineral's atomic network. Such observations suggest, that under a mixed radiation exposure like in the vicinity of nuclear reactor, a combination of neutrons and gamma rays could lead to a complex materials response, that requires further studies.

In the conducted research a decrease of compressive and flexural strength as well as dynamic modulus of elasticity in mortar after gamma irradiation (up to 1.6 MGy) was shown, respectively up to 10.3, 6.5 and 4.6%. Similar observations regarding the reduction of mechanical properties in the results of gamma irradiation were shown by Vodak et al. [38], despite the fact that the specimens were subjected to gamma irradiation of about 0.30 ÷ 0.55 MGy. Robira et al. [39] showed a decrease of the compressive strength by 3.6% between unirradiated and irradiated cement paste specimens after a total dose of 0.086 MGy. Similarly, a decrease by 18% was observed concerning the bending strength. Khmurovska et al. [41] revealed that the cement mortar strength was reduced about 20% under the exposure to gamma-ray irradiation with the total absorbed dose up to 15 MGy. On the other hand, Mobasher et al. [14] obtained an increase in the compressive strength of the mortar under gamma irradiation using 18,600 Gy/h. An explanation of such phenomenon is probably due to the gamma dose rate. The results of Soow and Milian [15] showed that for a given dose, cement mortar strength losses will be greater at lower dose rates. The effect of the gamma irradiation on the mechanical properties of cement based material varied with the radiation dose rate.

The linear correlation between carbonation depth and compressive strength and dynamic modulus of elasticity was also found, Figs. 10 and 11. In both cases, better fit was demonstrated for the irradiated specimens. This may be due to the influence of gamma radiation on the microstructure and porosity of the mortars. The porosity of concrete has been reported to decrease under irradiation [11], which would actually be advantageous for the durability of concrete to mass transfer weathering phenomena [38]. It has been proposed that because gamma radiation facilitates the formation of vaterite and aragonite (rather than calcite) during carbonation [18]. However, in the conducted research no traces of vaterite or aragonite were found, therefore it can be assumed that also calcite with increased hardness (Table 3) can have a similar effect.

6 Conclusions

Spent nuclear fuel in technological pool of research reactor was used as a source of long-term gamma radiation. Cement mortar carbonation and microstructural properties under gamma irradiation were experimentally investigated. The following conclusions can be drawn:

– Gamma irradiation up to 1.6 MGy resulted in accelerated carbonation of mortar with the

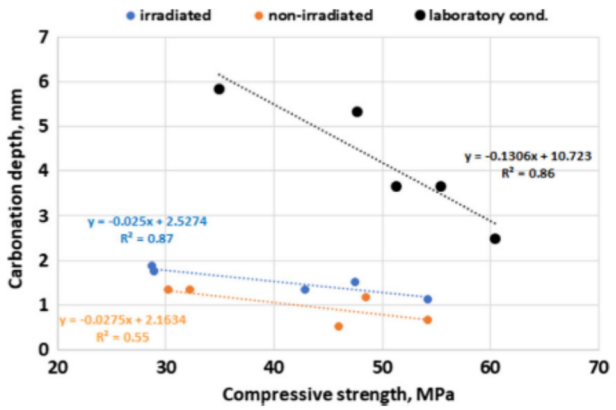

Fig. 10 Carbonation depth vs. compressive strength

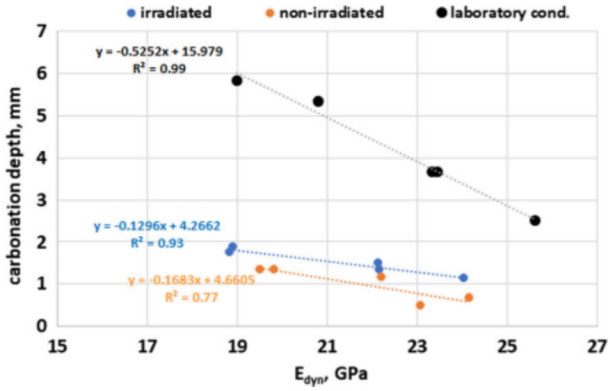

Fig. 11 Carbonation depth vs. dynamic modulus of elasticity

carbonation depth linearly increasing with increasing absorbed gamma dose. The correlation was valid for mortar without and with addition of limestone powder or fly ash.

- As a result of gamma irradiation a dense and homogeneous layer of calcite was found in irradiated mortar with limestone powder or fly ash, and only local carbonation in mortar stored in laboratory conditions. A higher content of calcite in gamma irradiated specimens was confirmed, but vaterite was not found.
- The carbonation products were significantly enlarged by γ irradiation. The size of calcite crystals was approx. 15 μm in contrast to 5 μm in non-irradiated specimens.
- Gamma irradiation substantially improved the micromechanical properties of products of carbonation. Calcite in irradiated mortar showed from six to eight times greater hardness. The Young's modulus of calcite was increased by 55% in mortar without mineral additives and by 13% in mortar with 40% fly ash.

Acknowledgements The financial support by The National Centre for Research and Development, Poland (Project V4-Korea/2/2018) is gratefully acknowledged.

Author's contribution DJN: Conceptualization, Data curation, Investigation, Methodology, Validation, Writing—original draft, Writing—review & editing. MD: Conceptualization, Investigation, Writing—review & editing. KD: Investigation, Writing—review & editing. DJ: Investigation, Validation, Writing—review & editing. AA: Investigation, Writing—review & editing. PD: Investigation, Writing—review & editing. MAG: Formal analysis, Funding acquisition, Methodology, Project administration, Supervision, Writing—review & editing.

Declarations

Conflict of interest The Authors declare that they have no known competing financial interests or personal relationships that could have appeared to influence the work reported in this paper.

References

1. Umeki Y, Sawada S, Mitsugi S, Maenaka T, Takiguchi K (2016) Outline of guidelines for maintenance and management of structures in nuclear facilities. J Adv Concr Technol 14(10):643–663. https://doi.org/10.3151/jact.14.643
2. Nauss DJ (2007) Primer on durability of nuclear power plant reinforced concrete structures - a review of pertinent factors, NUREG/CR-6927, ORNL/TM-2006/529. U.S. Nuclear Regulatory Commission, Washington, DC, p 128
3. Mitsugi S, Owaki E, Masuda H, Shimamoto R (2021) Accelerated concrete carbonation and resulting rebar corrosion under a high temperature condition in nuclear power plants. J Adv Concr Technol 19:382–394. https://doi.org/10.3151/jact.19.382
4. Leemann A, Moro F (2017) Carbonation of concrete - The role of CO_2 concentration, relative humidity and CO_2 buffer capacity. Mater Struct 50(30):30–43. https://doi.org/10.1617/s11527-016-0917-2
5. Shah V, Bishnoi S (2021) Understanding the process of carbonation in concrete using numerical modeling. J Adv Concr Technol 19:1148–1161. https://doi.org/10.3151/jact.19.1148
6. Pomaro B, Xotta G, Salomoni VA, Majorana CE (2022) A thermo-hydro-mechanical numerical model for plain irradiated concrete in nuclear shielding. Mater Struct 55(14):1–28. https://doi.org/10.1617/s11527-021-01844-1
7. Field KG, Remec I, Le Pape Y (2015) Radiation effects in concrete for nuclear power plants - Part I: quantification of radiation exposure and radiation effects. Nucl Eng Des 282:126–143. https://doi.org/10.1016/j.nucengdes.2014.10.003
8. Kontani O, Sawada S, Maruyama I, Takizawa M, Sato O (2013) Evaluation of irradiation effects on concrete structure: gamma-ray irradiation tests on cement paste. In: Proceedings of the ASME 2013 Power Conference. Volume 2: Reliability, Availability and Maintainability (RAM); Plant Systems, Structures, Components and Materials Issues; Simple and Combined Cycles; Advanced Energy Systems and Renewables (Wind, Solar and Geothermal); Energy Water Nexus; Thermal Hydraulics and CFD; Nuclear Plant Design, Licensing and Construction; Performance Testing and Performance Test Codes. Boston, Massachusetts, USA, V002T07A002. ASME. July 29–August 1, (2013). https://doi.org/10.1115/POWER2013-98099
9. Glinicki MA, Dąbrowski M, Antolik A, Dziedzic K, Sikorin S, Fateev V, Povolansky E (2022) Gamma irradiation sensitivity of early hardening cement mortar. Cem Concr Compos 126:104327. https://doi.org/10.1016/j.cemconcomp.2021.104327
10. Hunnicutt W, Tajuelo Rodriguez E, Mondal P, Le Pape Y (2020) Examination of gamma-irradiated calcium silicate

hydrates. Part II: mechanical properties. J Adv Concr Technol 18:558–570. https://doi.org/10.3151/jact.18.558
11. Reches Y (2019) A multi-scale review of the effects of gamma radiation on concrete. Results Mater 2:100039. https://doi.org/10.1016/j.rinma.2019.100039
12. Hilloulin B, Robira M, Loukili A (2018) Coupling statistical indentation and microscopy to evaluate micromechanical properties of materials: application to viscoelastic behavior of irradiated mortars. Cem Concr Compos 94:153–165. https://doi.org/10.1016/j.cemconcomp.2018.09.008
13. Soo P, Milian L (2001) The effect of gamma radiation on the strength of Portland cement mortars. J Mater Sci Lett 20(14):1345. https://doi.org/10.1023/A:1010971122496
14. Mobasher N, Bernal S, Kinoshita H, Sharrad C, Provis J (2015) Gamma irradiation resistance of an early age slag-blended cement matrix for nuclear waste encapsulation. J Mater Res 30(9):1563–1571. https://doi.org/10.1557/jmr.2014.404
15. Vodák F, Vydra V, Trtík K, Kapičková O (2011) Olga, Effect of gamma irradiation on properties of hardened cement paste. Mater Struct 44:101–107. https://doi.org/10.1617/s11527-010-9612-x
16. Bar-Nes G, Katz A, Peled Y, Zeiri Y (2008) The combined effect of radiation and carbonation on the immobilization of Sr and Cs ions in cementitious pastes. Mater Struct 41:1563. https://doi.org/10.1617/s11527-007-9348-4
17. Bykov GL, Abkhalimov EV, Ershov VA, Ershov BG (2021) Effect of gamma irradiation on Portland cement: hydrogen evolution and radiation resistance. Constr Build Mater 295:123644. https://doi.org/10.1016/j.conbuildmat.2021.123644
18. Maruyama I, Ishikawa S, Yasukouchi J, Sawada S, Kurihara R, Takizawa M, Kontani O (2018) Impact of gamma-ray irradiation on hardened white Portland cement pastes exposed to atmosphere. Cem Concr Res 108:59–71. https://doi.org/10.1016/j.cemconres.2018.03.005
19. Ashraf W (2016) Carbonation of cement-based materials: challenges and opportunities. Constr Build Mater 120:558–570. https://doi.org/10.1016/j.conbuildmat.2016.05.080
20. Liu P, Yu Z, Chen Y (2020) Carbonation depth model and carbonated acceleration rate of concrete under different environment. Cem Concr Compos 114:103736. https://doi.org/10.1016/j.cemconcomp.2020.103736
21. Morandeau A, Thiéry M, Dangla P (2015) Impact of accelerated carbonation on OPC cement paste blended with fly ash. Cem Concr Res 67:226–236. https://doi.org/10.1016/j.cemconres.2014.10.003
22. You X, Hu X, He P, Liu J, Shi C (2022) A review on the modelling of carbonation of hardened and fresh cement-based materials. Cem Concr Compos 125:104315. https://doi.org/10.1016/j.cemconcomp.2021.104315
23. Zajac M, Irbe L, Bullerjahn F, Hilbig H, Ben Haha M (2022) Mechanisms of carbonation hydration hardening in Portland cements. Cem Concr Res. 152:106687. https://doi.org/10.1016/j.cemconres.2021.106687
24. Kangni-Foli E, Poyet S, Le Bescop P, Charpentier T, Bernachy-Barbé F, Dauzères A, L'Hôpital E, d'Espinose de Lacaillerie J-B (2021) Carbonation of model cement pastes: the mineralogical origin of microstructural changes and shrinkage. Cem Concr Res 144:106446. https://doi.org/10.1016/j.cemconres.2021.106446
25. Potts A, Butcher E, Cann G, Leay D (2021) Long term effects of gamma irradiation on in-service concrete structures. J Nucl Mater 548:152868. https://doi.org/10.1016/j.jnucmat.2021.152868
26. Khmurovska Y, Štemberk P, Sikorin S, Němeček J, Jóźwiak-Niedźwiedzka D, Doleželová M, Kaladkevich Y, Pavalanski E, Fatseyeu V (2021) Effects of gamma-ray irradiation on hardened cement mortar. Int J Concr Struct Mater 15:17. https://doi.org/10.1186/s40069-020-00452-7
27. McDowall D, The effects of gamma radiation on the creep properties of concrete. In: Proceedings of an Information Exchange Meeting on Results of Concrete Irradiation Programmes, Brussels, Belgium, 19 April 1971. Brussels: Commission of the European Communities, Vol. EUR 4751 f-e, pp 55–69
28. PN-EN 196-1:2016-07, Methods of testing cement. Determination of strength, Polish Committee for Standardization (2016) p. 35
29. PN-EN 197-1: 2011 Cement - Composition, specifications and conformity criteria for common cements, Polish Committee for Standardization (2011) p. 21
30. PN-EN 450-1: 2012 Fly ash for concrete - Definition, specifications and conformity criteria, Polish Committee for Standardization (2012) p. 36
31. G. Krzysztoszek, The Characteristics and irradiation capabilities of MARIA research reactor in NCBJ Świerk. In: 2nd Int. Workshop Irradiation of Nuclear Materials: Flux and Dose Effects, November 4–6, 2015, CEA–INSTN Cadarache, France, EPJ Web of Conferences 115, 01004 (2016). https://doi.org/10.1051/epjconf/201611501004
32. Obryk B, Bilski P, Olko P (2011) Method of thermoluminescent measurement of radiation doses from micrograys up to a megagray with a single LiF:Mg,Cu,P detector. Radiat Prot Dosimetry 144(1–4):543–547
33. PN-EN 13295:2005, (2005) Products and systems for the protection and repair of concrete structures - test methods - determination of resistance to carbonation, Polish Committee for Standardization. p. 15
34. Oliver W, Pharr G (1992) An improved technique for determining hardness and elastic modulus using load and displacement sensing indentation experiments. J Mater Res 7:1564–1583. https://doi.org/10.1557/JMR.1992.1564
35. Spinner S, Teft WE (1961) A method for determining mechanical resonance frequencies and for calculating elastic modulus from these frequencies. Proc Amer Soc Testing Mat 61:1221–1238
36. Rathnarajan S, Dhanya BS, Pillai RG, Gettu R, Santhanam M (2021) Carbonation model for concretes with fly ash, slag, and limestone calcined clay - using accelerated and five - year natural exposure data. Cem Concr Compos 126:104329. https://doi.org/10.1016/j.cemconcomp.2021.104329
37. Jóźwiak-Niedźwiedzka D, Sobczak M, Gibas K (2013) Carbonation of concretes containing calcareous fly ashes. Roads Bridges - Drogi i Mosty 12(2):223–236. https://doi.org/10.7409/rabdim.013.016
38. Martín-García R, Alonso-Zarza AM, Frisia S, Rodríguez-Berriguete Á, Drysdale R, Hellstrom J (2019) Effect of aragonite to calcite transformation on the geochemistry and

dating accuracy of speleothems. An example from Castañar Cave, Spain. Sediment Geol 383:41–54. https://doi.org/10.1016/j.sedgeo.2019.01.014
39. Robira M, Hilloulin B, Loukili A, Potin G, Bourbon X, Abdelouas A (2018) Multi-scale investigation of the effect of γ irradiations on the mechanical properties of cementitious materials. Constr Build Mater 186:484–494. https://doi.org/10.1016/j.conbuildmat.2018.07.038
40. Vodák F, Trtík K, Sopko V, Kapičková O, Demo P (2005) Effect of γ-irradiation on strength of concrete for nuclear-safety structures. Cem Concr Res 35(7):1447–1451. https://doi.org/10.1016/j.cemconres.2004.10.016
41. Goñi S, Gaztañaga MT, Guerrero A (2002) Role of cement type on carbonation attack. J Mater Res 17:1834–1842. https://doi.org/10.1557/JMR.2002.0271
42. Dąbrowski M, Glinicki MA, Dziedzic K, Jóźwiak-Niedźwiedzka D, Sikorin S, Fateev VS, Povalansky EI (2021) Early age hardening of concrete with heavy aggregate in gamma radiation source – impact on the modulus of elasticity and microstructural features. J Adv Concr Technol 19(5):555–570. https://doi.org/10.3151/jact.19.555
43. Khmurovska Y, Štemberk P, Sikorin S, Žák J, Khaladkevich Y, Pavalanski E, Fatseyeu V (2019) Cement mortar creep under exposure to gamma-ray irradiation. J Nucl Research Dev 18:24–28
44. Velez K, Maximilien S, Damidot D, Fantozzi G, Sorrentino F (2001) Determination by nanoindentation of elastic modulus and hardness of pure constituents of Portland cement clinker. Cem Concr Res 31(4):555–561. https://doi.org/10.1016/S0008-8846(00)00505-6
45. Pomaro B (2016) A review on radiation damage in concrete for nuclear facilities: from experiments to modelling. Model Simul Eng 4165746:10. https://doi.org/10.1155/2016/4165746
46. Hughes JJ, Trtik P (2004) Micro-mechanical properties of cement paste measured by depth-sensing nanoindentation: a preliminary correlation of physical properties with phase type. Mater Charact 53(2–4):223–231. https://doi.org/10.1016/j.matchar.2004.08.014
47. Pignatelli I, Kumar A, Field K, Wang B, Yu Y, Le Pape Y, Bauchy M, Sant G (2016) Direct experimental evidence for differing reactivity alterations of minerals following irradiation: the case of calcite and quartz. Sci Rep 6:20155. https://doi.org/10.1038/srep20155